Matrix Completion Via Reweighted Logarithmic Norm Minimization

Zhijie Wang⬤, Liangtian He⬤, Qinghua Zhang⬤, Jifei Miao⬤, Liang-Jian Deng⬤, Jun Liu⬤

Abstract—**Low-rank matrix completion (LRMC) has demonstrated remarkable success in a wide range of applications. To address the NP-hard nature of the rank minimization problem, the nuclear norm is commonly used as a convex and computationally tractable surrogate for the rank function. However, this approach often yields suboptimal solutions due to the excessive shrinkage of singular values. In this letter, we propose a novel reweighted logarithmic norm as a more effective nonconvex surrogate, which provides a closer approximation than many existing alternatives. We efficiently solve the resulting optimization problem by employing the alternating direction method of multipliers (ADMM). Experimental results on image inpainting demonstrate that the proposed method achieves superior performance compared to state-of-the-art LRMC approaches, both in terms of visual quality and quantitative metrics.**

Index Terms—**Matrix completion, nuclear norm, low-rank approximation, nonconvex optimization, log-determinant.**

I. INTRODUCTION

RECOVERING the missing entries of a matrix from incomplete observations, known as matrix completion, has garnered considerable attention in various applications [1**? ?** –3]. Among these, low-rank matrix completion (LRMC) has demonstrated to be an effective technique. Current LRMC methods can be broadly categorized into two types. The first type employs the matrix factorization technique [4–8], which decomposes a matrix into the product of two or more smaller matrices to enhance computational efficiency. However, this approach typically requires pre-specifying the underlying rank, a task that can be challenging in practice.

The second type of LRMC methods is based on spectral regularization [9–12]. To avoid the NP-hard rank minimization problem, the nuclear norm is commonly adopted as a convex surrogate, leading to a computationally tractable nuclear norm minimization (NNM) problem [13]. However, the NNM applies uniform shrinkage to all singular values, which may lead to suboptimal solutions. Consequently, to more accurately approximate the rank function, a variety of nonconvex surrogate functions have been proposed in the literature, including the truncated nuclear norm [14], the weighted nuclear norm [15], the log-determinant heuristic [16–18], the Schatten capped p-norm [10], and the nuclear norm minus Frobenius norm [19], to mention just a few. These functions, in principle, penalize larger singular values less and smaller singular values more, and have empirically demonstrated superior performance compared to NNM.

Very recently, Chen et al. [20] proposed an efficient algorithm termed logarithmic norm regularized matrix factorization (LRMF), in which the authors introduced an effective matrix logarithmic norm (MLN) and combined it with bi-factor and multi-factor strategies to enhance computational efficiency. However, the LRMF method is restricted to specific values of p, that is, $p = \frac{1}{n}$, where $n = 1, 2, \cdots$.

In this letter, to make the MLN surrogate proposed in [20] a better approximation of the rank function, we propose a novel *reweighted* matrix logarithmic norm (RMLN). Additionally, we develop an iterative optimization algorithm within the framework of the alternating direction method of multipliers (ADMM), which enables our proposed method to be applicable to any $0 < p \leqslant 1$. The main contributions of this work are summarized as follows.

- We propose a novel reweighted matrix logarithmic norm regularization, which provides a more accurate approximation to the rank function.
- The resulting optimization problem is solved within the ADMM framework. In contrast to the LRMF algorithm proposed in [20], our approach is applicable to any $p \in (0, 1]$, thereby removing the restriction to specific values.
- Extensive experiments on image inpainting demonstrate the superior recovery performance of our proposed method compared to state-of-the-art LRMC approaches.

II. PRELIMINARIES

A. Notations

Throughout this letter, $\mathbb{R}$ denotes the real space. Scalars, vectors, and matrices are denoted by x, $\mathbf{x}$, and $\mathbf{X}$, respectively. Standard operations include $(\cdot)^{-1}$ for the matrix inversion and $(\cdot)^T$ for the transposition. The Frobenius norm and the nuclear norm are denoted by $||\cdot||_F$ and $||\cdot||_*$, respectively. Additionally, $\det(\cdot)$ represents the matrix determinant, and $tr(\cdot)$ denotes the matrix trace.

B. LRMC Problem

The LRMC problem aims to recover the underlying matrix $\mathbf{X} \in \mathbb{R}^{M \times N}$ from its partially observed entries in $\mathbf{Y}$, indexed by the set Ω. This problem can be formulated as:

$$\min_{\mathbf{X}} \text{rank}(\mathbf{X}) \quad \text{s.t.} \quad \mathcal{P}_\Omega(\mathbf{X} - \mathbf{Y}) = \mathbf{0}, \quad (1)$$

where $\text{rank}(\cdot)$ denotes the rank of a matrix. The projection operator $\mathcal{P}_\Omega : \mathbb{R}^{M \times N} \to \mathbb{R}^{M \times N}$ is defined as:

$$(\mathcal{P}_\Omega(\mathbf{X}))_{i,j} = \begin{cases} \mathbf{X}_{i,j}, & (i,j) \in \Omega, \\ 0, & (i,j) \in \Omega^c, \end{cases} \quad (2)$$

where $\mathbf{X}_{i,j}$ denotes the entry at position (i,j), and Ω^c represents the complement of the set Ω.

However, the optimization problem specified in Eq. (1) is NP-hard, owing to the non-convexity and discontinuity inherent in the rank function. To tackle this intractability, the nuclear norm is commonly employed as a convex surrogate. It is formally defined as the sum of singular values, i.e., $||\mathbf{X}||_* = \sum_{i=1}^{\min\{M,N\}} \sigma_i(\mathbf{X})$, where $\sigma_i(\mathbf{X})$ denotes the i-th singular value of $\mathbf{X}$. A key justification for its use is that it constitutes the tightest convex envelope of the rank function. This leads to the nuclear norm minimization (NNM) recovery formulation:

$$\min_{\mathbf{X}} ||\mathbf{X}||_* \quad \text{s.t.} \quad \mathcal{P}_\Omega(\mathbf{X} - \mathbf{Y}) = \mathbf{0}. \quad (3)$$

While NNM renders the optimization problem computationally tractable [13, 21], a notable drawback is its tendency to excessively shrink larger singular values. This bias often leads to suboptimal solutions and thus motivates the search for more precise nonconvex surrogates that can better approximate the rank function.
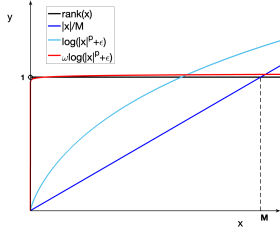
Fig. 1: Comparison of the rank function, the convex envelope of rank (nuclear norm) [13], the MLN [20], and the proposed RMLN for scalar x.

C. Matrix Logarithmic Norm

Motivated by the log-determinant heuristic $\log\det(\mathbf{X} + \varepsilon\mathbf{I})$ [18], Chen et al. [20] introduced the matrix logarithmic norm (MLN) as a nonconvex surrogate for the rank function.

Definition 1. (MLN [20]) *Given a matrix* $\mathbf{X} \in \mathbb{R}^{M \times N}$, *the MLN of* $\mathbf{X}$ *is defined as:*

$$||\mathbf{X}||_L^p := \sum_{i=1}^{\min\{M,N\}} \log(\sigma_i^p(\mathbf{X}) + \varepsilon), \qquad (4)$$

where $\sigma_i(\mathbf{X})$ *denotes the* i-th singular value of $\mathbf{X}$.

To facilitate optimization, the authors derived both bi-factor and multi-factor matrix factorization forms for the MLN and subsequently employed a block-coordinate descent algorithm to efficiently solve the resulting minimization problem. A notable restriction of this approach, however, is that the parameter p is restricted to specific discrete values, namely $p = \frac{1}{n}$ for $n = 1, 2, \cdots$. For comprehensive algorithmic details, the interested readers are referred to [20].

III. THE PROPOSED METHOD

A. Reweighted Matrix Logarithmic Norm

Drawing inspiration from the success of reweighting strategies [5, 22, 23] and the effective rank approximation provided by the MLN [20], we propose the *reweighted* matrix logarithmic norm (RMLN). This new surrogate function is formally defined as follows.

Definition 2. (RMLN) *Given a matrix* $\mathbf{X} \in \mathbb{R}^{M \times N}$, *the RMLN of* $\mathbf{X}$ *is defined as:*

$$||\mathbf{X}||_{\mathbf{w},L}^p := \sum_{i=1}^{\min\{M,N\}} w_i \log(\sigma_i^p(\mathbf{X}) + \varepsilon), \qquad (5)$$

where the weights are given by:

$$w_i = \gamma \left(\log(\sigma_i^p(\mathbf{X}) + \varepsilon) + c \right)^{p-1}, \ 0 < p \leqslant 1, \qquad (6)$$

where c, γ, *and* ε *are positive constants.*

Fig. 1 provides an intuitive comparison of the rank function, the nuclear norm, the MLN [20], and the proposed RMLN in the scalar case, where $\mathbf{X} = x \in \mathbb{R}$. For a scalar x bounded by M (i.e., $|x| \leqslant M$), then $\frac{||\mathbf{X}||_*}{M} = \frac{|x|}{M}$ forms the convex envelope of the rank function [20, 24], and the MLN and RMLN are given by $||\mathbf{X}||_L^p = \log(|x|^p + \varepsilon)$ and $||\mathbf{X}||_{\mathbf{w},L}^p = w\log(|x|^p + \varepsilon)$, respectively. As observed, our proposed RMLN exhibits a behavior that closely approximates the rank function, which highlights its superior capability for rank approximation.

B. RMLN for Matrix Completion

We employ the proposed RMLN as a spectral regularization and formulate the matrix completion problem as follows:

$$\min_{\mathbf{X}} \lambda ||\mathbf{X}||_{\mathbf{w},L}^p + \frac{1}{2}||\mathcal{P}_\Omega(\mathbf{X} - \mathbf{Y})||_F^2. \qquad (7)$$

To solve this optimization problem, we adopt the ADMM [25]. Specifically, by introducing an auxiliary variable $\mathbf{Z}$, it allows us to reformulate the original problem (7) into an equivalent constrained form:

$$\min_{\mathbf{X},\mathbf{Z}} \lambda ||\mathbf{Z}||_{\mathbf{w},L}^p + \frac{1}{2}||\mathcal{P}_\Omega(\mathbf{X} - \mathbf{Y})||_F^2, \quad s.t. \quad \mathbf{Z} = \mathbf{X}. \qquad (8)$$

The corresponding augmented Lagrangian for this constrained problem is given by:

$$\mathcal{L}_\mu(\mathbf{X}, \mathbf{Z}, \mathbf{\Lambda}) = \frac{1}{2}||\mathcal{P}_\Omega(\mathbf{X}-\mathbf{Y})||_F^2 + \lambda||\mathbf{Z}||_{\mathbf{w},L}^p + \frac{\mu}{2}||\mathbf{Z}-\mathbf{X}-\frac{\mathbf{\Lambda}}{\mu}||_F^2, \qquad (9)$$

where $\mu > 0$ is a penalty parameter and $\mathbf{\Lambda}$ is the Lagrangian multiplier. The ADMM algorithm then proceeds by iteratively minimizing $\mathcal{L}_\mu$ with respect to $\mathbf{X}$ and $\mathbf{Z}$ alternately, while updating the multiplier $\mathbf{\Lambda}$.

In the k-th iteration, with the other variables fixed, this procedure yields the following update rules.

1) Updating $\mathbf{X}$:

$$\mathbf{X}^{(k+1)} = \arg\min_{\mathbf{X}} \frac{1}{2}||\mathcal{P}_\Omega(\mathbf{X}-\mathbf{Y})||_F^2 + \frac{\mu^{(k)}}{2}||\mathbf{X}+\frac{\mathbf{\Lambda}^{(k)}}{\mu^{(k)}}-\mathbf{Z}^{(k)}||_F^2. \qquad (10)$$

Applying the first-order optimality condition yields a closed-form solution:

$$\mathbf{X}^{(k+1)} = \mathcal{P}_{\Omega^c}\left(\mathbf{Z}^{(k)} - \frac{\mathbf{\Lambda}^{(k)}}{\mu^{(k)}}\right) + \mathcal{P}_\Omega\left(\frac{\mathbf{Y}+\mu^{(k)}\mathbf{Z}^{(k)}-\mathbf{\Lambda}^{(k)}}{1+\mu^{(k)}}\right). \qquad (11)$$

2) Updating $\mathbf{Z}$:

$$\mathbf{Z}^{(k+1)} = \arg\min_{\mathbf{Z}} \frac{\mu^{(k)}}{2}||\mathbf{Z}-\mathbf{X}^{(k+1)}-\frac{\mathbf{\Lambda}^{(k)}}{\mu^{(k)}}||_F^2 + \lambda||\mathbf{Z}||_{\mathbf{w},L}^p. \qquad (12)$$

Before deriving the solution to Eq. (12), we first present the following theorem.

Theorem 1. *Let* $\mathbf{Y} \in \mathbb{R}^{M \times N}$ *be any matrix with singular value decomposition* $\mathbf{Y} = \mathbf{U_Y}\mathbf{\Sigma_Y}\mathbf{V_Y}^T$, *where* $\mathbf{\Sigma_Y} = diag(\sigma_1(\mathbf{Y}), \sigma_2(\mathbf{Y}), \cdots, \sigma_{\min\{M,N\}}(\mathbf{Y}))$. *For any* $\eta > 0$, *the optimal solution to the following optimization problem:*

$$\arg\min_{\mathbf{X}} \frac{1}{2}||\mathbf{X}-\mathbf{Y}||_F^2 + \eta||\mathbf{X}||_{\mathbf{w},L}^p \qquad (13)$$

is given by $\mathbf{X}^* = \mathbf{U_Y}\mathbf{\Sigma_X^*}\mathbf{V_Y}^T$. *Here, the singular value matrix* $\mathbf{\Sigma_X^*} = diag(\sigma_1^*(\mathbf{X}), \sigma_2^*(\mathbf{X}), \cdots, \sigma_{\min\{M,N\}}^*(\mathbf{X}))$ *and the optimal singular values* $\sigma_i^*(\mathbf{X})$ *are obtained by:*

$$\sigma_i^*(\mathbf{X}) = \arg\min_{\sigma_i(\mathbf{X})\geqslant 0} \frac{1}{2}(\sigma_i(\mathbf{X}) - \sigma_i(\mathbf{Y}))^2 + \eta w_i \log(\sigma_i^p(\mathbf{X}) + \varepsilon), \qquad (14)$$

where $i = 1, 2, \cdots, \min\{M, N\}$.

Proof. *Let* $\mathbf{Y} = \mathbf{U_Y}\mathbf{\Sigma_Y}\mathbf{V_Y}^T$ *be the SVD of* $\mathbf{Y} \in \mathbb{R}^{M \times N}$. *Then, we have:*

$$\frac{1}{2}||\mathbf{X}-\mathbf{Y}||_F^2 + \eta||\mathbf{X}||_{\mathbf{w},L}^p$$
$$= \frac{1}{2}\left(tr(\mathbf{Y}^T\mathbf{Y}) + tr(\mathbf{X}^T\mathbf{X}) - 2tr(\mathbf{X}^T\mathbf{Y})\right) + \eta||\mathbf{X}||_{\mathbf{w},L}^p$$
$$= \frac{1}{2}\left(\sum_i \sigma_i^2(\mathbf{Y}) + \sum_i \sigma_i^2(\mathbf{X}) - 2tr(\mathbf{X}^T\mathbf{Y})\right) + \eta||\mathbf{X}||_{\mathbf{w},L}^p$$
$$\geqslant \frac{1}{2}\sum_i \left(\sigma_i^2(\mathbf{Y}) + \sigma_i^2(\mathbf{X}) - 2\sigma_i(\mathbf{Y})\sigma_i(\mathbf{X})\right) + \eta||\mathbf{X}||_{\mathbf{w},L}^p$$
$$= \sum_i \frac{1}{2}(\sigma_i(\mathbf{Y}) - \sigma_i(\mathbf{X}))^2 + \eta w_i \log(\sigma_i^p(\mathbf{X}) + \varepsilon),$$

in which the inequality follows from Von Neumann's trace inequality [26]. Therefore, the optimal solution to Eq. (13) is given by $\mathbf{X}^* = \mathbf{U_Y}\mathbf{\Sigma_X^*}\mathbf{V_Y}^T$. ∎

According to Theorem 1, the problem in Eq. (13) is equivalent to solving Eq. (14). Note that the function $w \log(|x|^{\tilde{p}} + \varepsilon)$ is concave, monotonically increasing, and continuously differentiable on $[0, +\infty)$ These properties render the problem Eq. (14) amenable to the difference of convex (DC) algorithm [27]. Specifically, the DC algorithm proceeds by iteratively linearizing the concave part of the objective function, while leaving the convex quadratic ℓ_2-norm term unchanged. This results in the following iterative update for each singular value:

$$\sigma_i^{(t+1)}(\mathbf{X}) = \arg \min_{\sigma_i(\mathbf{X}) \geqslant 0} \frac{1}{2}(\sigma_i(\mathbf{X}) - \sigma_i(\mathbf{Y}))^2 + \frac{\eta w_i p(\sigma_i^{(t)}(\mathbf{X}))^{p-1} \sigma_i}{(\sigma_i^{(t)}(\mathbf{X}))^p + \varepsilon}, \tag{15}$$

where $i = 1, 2, \cdots, \min\{M, N\}$, and the superscript t is the iteration index.

A closed-form solution for Eq. (15) can be derived by applying the first-order optimality condition, leading to the final update rule:

$$\sigma_i^{(t+1)}(\mathbf{X}) = \max \left\{ \sigma_i(\mathbf{Y}) - \frac{\eta w_i p(\sigma_i^{(t)}(\mathbf{X}))^{p-1}}{(\sigma_i^{(t)}(\mathbf{X}))^p + \varepsilon}, 0 \right\}. \tag{16}$$

3) Updating $\mathbf{\Lambda}$ *and* μ:

$$\begin{cases} \mathbf{\Lambda}^{(k+1)} = \mathbf{\Lambda}^{(k)} + \mu^{(k)}(\mathbf{X}^{(k+1)} - \mathbf{Z}^{(k+1)}), \\ \mu^{(k+1)} = \mu^{(k)} \cdot \rho \quad (\rho > 1). \end{cases} \tag{17}$$

For clarity, the complete procedure for the proposed RMLN regularization based matrix completion is detailed in Algorithm 1.

Algorithm 1 RMLN minimization for matrix completion.

Input: Incomplete matrix $\mathbf{Y} \in \mathbb{R}^{M \times N}$, the set of observed entries Ω, $\mu^{(0)}$, ρ, γ, λ, p, ε, c, K and T.
1: **Initialize:** $\mathbf{X}^{(0)} = \mathbf{Z}^{(0)} = \mathbf{Y}$, $\mathbf{\Lambda}^{(0)} = \mathbf{0}$.
2: **for** $k = 0, 1, \cdots, K$ **do**
3: Update $\mathbf{X}^{(k+1)}$ by Eq. (10).
4: Update $\mathbf{Z}^{(k+1)}$ by Eq. (12) based on Theorem 1.
5: **for** $i = 1, 2, \cdots, \min\{M, N\}$ **do**
6:   Update $w_i = \gamma \left(\log(\sigma_i^p(\mathbf{Z}^{(k)}) + \varepsilon) + c\right)^{p-1}$.
7:   $\sigma_i^{(0)}(\mathbf{Z}^{(k+1)}) = \sigma_i(\mathbf{Z}^{(k)})$.
8:   **for** $t = 0, 1, \cdots, T$ **do**
9:    Update $\sigma_i^{(t+1)}(\mathbf{Z}^{(k+1)}) = \max\{(\sigma_i(\mathbf{X}^{(k+1)} + \frac{\mathbf{\Lambda}^{(k)}}{\mu^{(k)}}) - \frac{\lambda w_i p(\sigma_i^{(t)}(\mathbf{Z}^{(k+1)}))^{p-1}}{\mu^{(k)}((\sigma_i^{(t)}(\mathbf{Z}^{(k+1)}))^p + \varepsilon)}, 0\}$.
10:   **end for**
11: **end for**
12: Update $\mathbf{\Lambda}^{(k+1)}$ and $\mu^{(k+1)}$ by Eq. (17).
13: $k \leftarrow k + 1$.
14: **end for**
Output: The completed matrix $\mathbf{X}^{(K)}$.

IV. NUMERICAL EXPERIMENTS

In this section, we conduct comprehensive numerical experiments to validate the efficacy of our proposed method. To quantitatively assess the reconstruction quality, we employ two widely used metrics: the peak signal-to-noise ratio (PSNR) and the structural similarity index (SSIM) [28]. All experiments were performed in Matlab 2021b with an Intel Core i7-14700KF processor (3.40 GHz), 32 GB of RAM. Due to space limitations, more experiments can be found in the Supplemental Material.
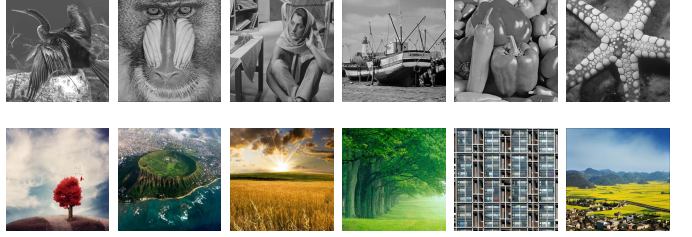

Fig. 2: The Set12 dataset. The test images from left-to-right and top-to-bottom are labeled as Img1 to Img12, respectively.

A. Experimental Setup

We compare the proposed RMLN algorithm against several state-of-the-art approaches, categorized as follows:
- **Spectral regularization-based methods:** Geman [29], TNNR (solved via ADMM) [14], WNNM [15], SCp [10], and NMF [19].
- **Matrix factorization-based methods:** D-N [4], F-N [4], and LRMF ($n = 2$) [20].

Our evaluation is conducted on two datasets: Set12 (illustrated in Fig. 2) and the benchmark BSD68 [30]. Following prior works [10, 20], color images are processed individually for each channel. Our specific parameter settings are as follows: $\lambda = 3 \times 10^5$, $\varepsilon = 800$, $\mu^{(0)} = 10^{-3}$, $\rho = 1.1$, $\gamma = 10$, $c = 10^{-8}$, $p = 0.8$, $K = 100$ and $T = 5$. To ensure a fair comparison, the parameters for all competing methods were either adopted directly from their original publications or carefully tuned to achieve optimal performance.

B. Random Mask Experiments

We evaluate the performance under random mask scenarios at missing ratios (MRs) of 0.50, 0.65, and 0.75. Intuitively, a higher MR value corresponds to a more challenging matrix completion task. The quantitative results, presented in Table I, show that our proposed method consistently outperforms other approaches in terms of both PSNR and SSIM across all MR settings. For a qualitative assessment, Figs. 3 and 4 provide visual comparisons. In contrast to the competing methods, our algorithm produces reconstructions with superior clarity and effectively suppresses undesirable artifacts.

C. Block Mask Experiments

To further evaluate the generalization capability of our method, we conducted experiments under a more challenging scenario involving block masks. Specifically, we applied rectangular occlusion patterns to the test image "Img11". As illustrated in Fig. 5, the visual comparison reveals that existing approaches struggle with this task, either failing to recover structural integrity or producing severe visual artifacts. In contrast, our proposed method demonstrates superior performance by effectively preserving fine details and significantly reducing unpleasant artifacts.

D. Role of The Reweighted Strategy

To investigate the impact of different weighting schemes on the recovery performance, we present a comparative numerical analysis in Table II. We evaluate three distinct weighting methods: uniform weights $w_i^{\mathbf{a}} = 1$, logarithmic-based weights $w_i^{\mathbf{b}} = \gamma \left(\log(\sigma_i^p(\mathbf{X}) + \varepsilon) + c\right)^{-1}$ and the reweighted strategy $w_i^{\mathbf{c}} = \gamma \left(\log(\sigma_i^p(\mathbf{X}) + \varepsilon) + c\right)^{p-1}$. The results in Table II demonstrate that the reweighted strategy achieves the highest performance metrics.

TABLE I: Average PSNR (dB) and SSIM values of compared methods at different missing ratios (MR = 0.50, 0.65, and 0.75) on the Set12 and BSD68 datasets. Best results are highlighted in **bold**.

Methods	D-N [4]	F-N [4]	Geman [29]	TNNR [14]	WNNM [15]	SCp [10]	NMF [19]	LRMF [20]	RMLN (ours)
Set12									
MR = 0.50									
PSNR	24.84	25.04	25.01	25.13	24.94	25.01	25.48	25.64	**26.74**
SSIM	0.7986	0.7996	0.8029	0.8119	0.7899	0.8007	0.8048	0.8147	**0.8511**
MR = 0.65									
PSNR	22.54	22.94	22.83	22.96	22.77	22.73	23.13	23.40	**24.24**
SSIM	0.7099	0.7091	0.7143	0.7180	0.6986	0.7061	0.7079	0.7260	**0.7581**
MR = 0.75									
PSNR	20.79	21.14	21.13	21.16	20.92	21.01	21.38	21.64	**22.40**
SSIM	0.6226	0.6268	0.6417	0.6339	0.6155	0.6269	0.6284	0.6417	**0.6768**
BSD68									
MR = 0.50									
PSNR	24.48	25.13	25.10	25.63	24.73	24.89	25.49	25.51	**26.80**
SSIM	0.7008	0.7215	0.7158	0.7396	0.7021	0.7084	0.7227	0.7272	**0.7818**
MR = 0.65									
PSNR	22.96	23.31	22.95	23.05	22.64	22.69	23.25	23.24	**24.33**
SSIM	0.6069	0.6142	0.6026	0.6031	0.5837	0.5943	0.6001	0.6134	**0.6563**
MR = 0.75									
PSNR	21.50	21.69	21.41	21.17	21.09	20.21	21.64	21.68	**22.59**
SSIM	0.5170	0.5101	0.5128	0.4904	0.4847	0.5032	0.4997	0.5225	**0.5486**

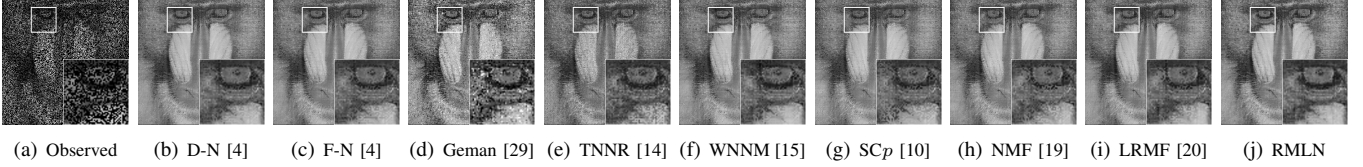(a) Observed   (b) D-N [4]   (c) F-N [4]   (d) Geman [29]   (e) TNNR [14]   (f) WNNM [15]   (g) SCp [10]   (h) NMF [19]   (i) LRMF [20]   (j) RMLN

Fig. 3: The visual quality of different methods on image "Img2" from the Set12 dataset with a random mask (MR = 0.50).

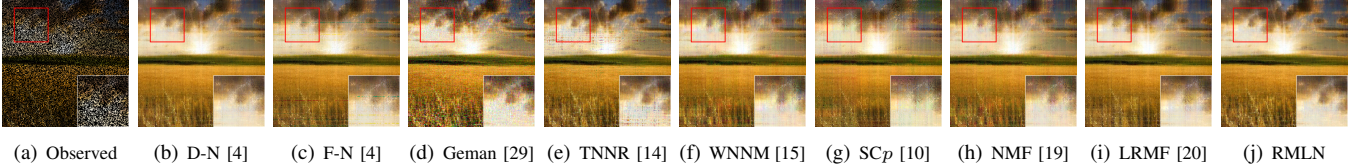(a) Observed   (b) D-N [4]   (c) F-N [4]   (d) Geman [29]   (e) TNNR [14]   (f) WNNM [15]   (g) SCp [10]   (h) NMF [19]   (i) LRMF [20]   (j) RMLN

Fig. 4: The visual quality of different methods on image "Img9" from the Set12 dataset with a random mask (MR = 0.65).
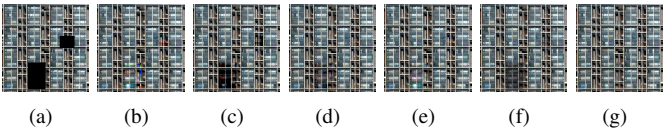

(a)   (b)   (c)   (d)   (e)   (f)   (g)

Fig. 5: The visual quality and SSIM values of different methods on image "Img11" from the Set12 dataset with block masks. (a) Observed image; (b) Geman [29] (0.9712); (c) TNNR [14] (0.9412); (d) WNNM [15] (0.9663); (e) SCp [10] (0.9736); (f) NMF [19] (0.9658); (g) RMLN (**0.9842**).

TABLE II: Average PSNR (dB) and SSIM values for different weight strategies on the Set12 dataset.

Weights	MR = 0.50	MR = 0.65	MR = 0.75
$w_i^{\mathbf{a}}$	26.03/0.8092	23.66/0.7267	21.82/0.6390
$w_i^{\mathbf{b}}$	26.59/0.8463	24.10/0.7510	22.21/0.6673
$w_i^{\mathbf{c}}$	26.74/0.8511	24.24/0.7581	22.40/0.6768

E. Analysis of Power p

This subsection investigates the impact of the power parameter p within our RMLN minimization framework. Fig. 6 illustrates the PSNR values across various MRs as p varies
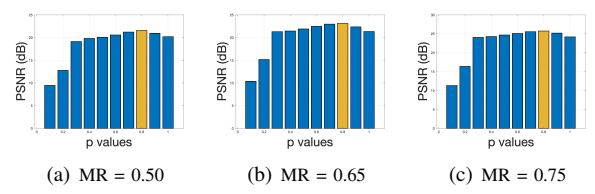

(a) MR = 0.50   (b) MR = 0.65   (c) MR = 0.75

Fig. 6: The effect of varying p on "Img1" under different MRs.

from 0.1 to 1. The results indicate that our method is relatively insensitive to the choice of p, and empirically, $p = 0.8$ is identified as the optimal value.

V. CONCLUSION

This letter introduces a novel reweighted matrix logarithmic norm (RMLN) regularization for matrix completion. The RMLN formulation provides a more accurate approximation to the rank function. Extensive experiments on image inpainting demonstrate that our method achieves superior recovery performance over existing approaches in terms of both quantitative metrics and visual quality. Future work will extend the RMLN framework to other relevant tasks, including matrix completion with noise corruption [31**?**] and robust principal component analysis [4].

References

[1] X. Jiang, Z. Zhong, X. Liu, and H. C. So, "Robust matrix completion via alternating projection," *IEEE Signal Process. Lett.*, vol. 24, no. 5, pp. 579–583, 2017.

[2] X. P. Li, Q. Liu, and H. C. So, "Rank-one matrix approximation with ℓ_p-norm for image inpainting," *IEEE Signal Process. Lett.*, vol. 27, pp. 680–684, 2020.

[3] H. Fathi, E. Rangriz, and V. Pourahmadi, "Two novel algorithms for low-rank matrix completion problem," *IEEE Signal Process. Lett.*, vol. 28, pp. 892–896, 2021.

[4] F. Shang, J. Cheng, Y. Liu, Z. Q. Luo, and Z. Lin, "Bilinear factor matrix norm minimization for robust PCA: Algorithms and applications," *IEEE Trans. Pattern Anal. Mach. Intell.*, vol. 40, no. 9, pp. 2066–2080, 2018.

[5] L. Chen, X. Jiang, X. Liu, and M. Haardt, "Reweighted low-rank factorization with deep prior for image restoration," *IEEE Trans. Signal Process.*, vol. 70, pp. 3514–3529, 2022.

[6] Z. Wen, W. Yin, and Y. Zhang, "Solving a low-rank factorization model for matrix completion by a nonlinear successive over-relaxation algorithm," *Math Program Comput.*, vol. 4, no. 4, pp. 333–361, 2012.

[7] R. Ma, N. Barzigar, A. Roozgard, and S. Cheng, "Decomposition approach for low-rank matrix completion and its applications," *IEEE Trans. Signal Process.*, vol. 62, no. 7, pp. 1671–1683, 2014.

[8] Y. Chi, Y. M. Lu, and Y. Chen, "Nonconvex optimization meets low-rank matrix factorization: An overview," *IEEE Trans. Signal Process.*, vol. 67, no. 20, pp. 5239–5269, 2019.

[9] C. Lu, J. Tang, S. Yan, and Z. Lin, "Generalized nonconvex nonsmooth low-rank minimization," in *Proc. IEEE Conf. Comput. Vis. Pattern Recognit.* CVPR, 2014, pp. 4130–4137.

[10] G. Li, G. Guo, S. Peng, C. Wang, S. Yu, J. Niu, and J. Mo, "Matrix completion via schatten capped p norm," *IEEE Trans. Knowl. Data Eng.*, vol. 34, no. 1, pp. 394–404, 2020.

[11] F. Nie, H. Huang, and C. H. Q. Ding, "Low-rank matrix recovery via efficient Schatten p-norm minimization," in *Proc. AAAI Conf. Artif. Intell.*, 2012, pp. 22–26.

[12] F. Nie, Z. Hu, and X. Li, "Matrix completion based on non-convex low-rank approximation," *IEEE Trans. Image Process.*, vol. 28, no. 5, pp. 2378–2388, 2019.

[13] J.-F. Cai, E. J. Candès, and Z. Shen, "A singular value thresholding algorithm for matrix completion," *SIAM J. Control.*, vol. 20, no. 4, pp. 1956–1982, 2010.

[14] Y. Hu, D. Zhang, J. Ye, X. Li, and X. He, "Fast and accurate matrix completion via truncated nuclear norm regularization," *IEEE Trans. Pattern Anal. Mach. Intell.*, vol. 35, no. 9, pp. 2117–2130, 2013.

[15] S. Gu, Q. Xie, D. Meng, W. Zuo, X. Feng, and L. Zhang, "Weighted nuclear norm minimization and its applications to low level vision," *Int. J. Comput. Vis.*, vol. 121, no. 2, pp. 183–208, 2017.

[16] C. Yang, X. Shen, H. Ma, B. Chen, Y. Gu, and H. C. So, "Weakly convex regularized robust sparse recovery methods with theoretical guarantees," *IEEE Trans. Signal Process.*, vol. 67, no. 19, pp. 5046–5061, 2019.

[17] L. Chen and Y. Gu, "The convergence guarantees of a non-convex approach for sparse recovery," *IEEE Trans. Signal Process.*, vol. 62, no. 15, pp. 3754–3767, 2014.

[18] Z. Kang, C. Peng, and Q. Cheng, "Top-n recommender system via matrix completion," in *Proc. AAAI Conf. Artif. Intell.*, vol. 30, no. 1, 2016.

[19] Y. Shan, D. Hu, Z. Wang, and T. Jia, "Multi-channel nuclear norm minus Frobenius norm minimization for color image denoising," *Signal Process.*, vol. 207, p. 108959, 2023.

[20] L. Chen, X. Jiang, X. Liu, and Z. Zhou, "Logarithmic norm regularized low-rank factorization for matrix and tensor completion," *IEEE Trans. Image Process.*, vol. 30, pp. 3434–3449, 2021.

[21] T.-H. Oh, Y. Matsushita, Y.-W. Tai, and I. S. Kweon, "Fast randomized singular value thresholding for low-rank optimization," *IEEE Trans. Pattern Anal. Mach. Intell.*, vol. 40, no. 2, pp. 376–391, 2018.

[22] Y. Xie, S. Gu, Y. Liu, W. Zuo, W. Zhang, and L. Zhang, "Weighted schatten p-norm minimization for image denoising and background subtraction," *IEEE Trans. Image Process.*, vol. 25, no. 10, pp. 4842–4857, 2016.

[23] Y. Huang, G. Liao, Y. Xiang, L. Zhang, J. Li, and A. Nehorai, "Low-rank approximation via generalized reweighted iterative nuclear and Frobenius norms," *IEEE Trans. Image Process.*, vol. 29, pp. 2244–2257, 2020.

[24] M. Fazel, H. Hindi, and S. P. Boyd, "A rank minimization heuristic with application to minimum order system approximation," in *Proc. Amer. Control Conf.*, vol. 6. IEEE, 2001, pp. 4734–4739.

[25] S. P. Boyd, N. Parikh, E. Chu, B. Peleato, and J. Eckstein, "Distributed optimization and statistical learning via the alternating direction method of multipliers," *Found. Trends Mach. Learn.*, vol. 3, no. 1, pp. 1–122, 2011.

[26] L. Mirsky, "A trace inequality of john von neumann," *Monatshefte für math.*, vol. 79, no. 4, pp. 303–306, 1975.

[27] P. D. Tao and L. H. An, "Convex analysis approach to DC programming: theory, algorithms and applications," *Acta Math. Vietnam.*, vol. 22, no. 1, pp. 289–355, 1997.

[28] Z. Wang, A. C. Bovik, H. R. Sheikh, and E. P. Simoncelli, "Image quality assessment: From error visibility to structural similarity," *IEEE Trans. Image Process.*, vol. 13, no. 4, pp. 600–612, 2004.

[29] Z. Kang, C. Peng, and Q. Cheng, "Robust PCA via nonconvex rank approximation," in *Proc. IEEE Int. Conf. Data Min.* IEEE, 2015, pp. 211–220.

[30] D. Martin, C. Fowlkes, D. Tal, and J. Malik, "A database of human segmented natural images and its application to evaluating segmentation algorithms and measuring ecological statistics," in *Proc. IEEE Int. Conf. Comput. Vis.*, vol. 2, 2001, pp. 416–423.

[31] E. J. Candès and Y. Plan, "Matrix completion with noise," *Proc. IEEE*, vol. 98, no. 6, pp. 925–936, 2010.